

## Influence of temperature on air runoff in the propagation of a forest fire

Inês Gonçalves<sup>1</sup>, João Marques<sup>2</sup>, João Silva<sup>3</sup>, José Teixeira<sup>4</sup>, Filipe Alvelos<sup>5</sup>, Senhorinha Teixeira<sup>6</sup>

<sup>1</sup>ALGORITMI, University of Minho, Portugal. Email: b12799@algoritmi.uminho.pt

<sup>2</sup>ALGORITMI, University of Minho, Portugal. Email: b12802@algoritmi.uminho.pt

<sup>3</sup>ALGORITMI, University of Minho, Portugal Email: js@dem.uminho.pt

<sup>4</sup>ALGORITMI, University of Minho, Portugal Email: jt@dem.uminho.pt

<sup>5</sup>ALGORITMI, University of Minho, Portugal Email: falvelos@dps.uminho.pt

<sup>6</sup>ALGORITMI, University of Minho, Portugal Email: st@dps.uminho.pt

Wildfires are a worldwide phenomenon that endangers the ecosystems and all its surroundings. Because forest fires are unpredictable phenomena, it is critical to maximize the instruments employed to mitigate their harmful effects. The main purpose of this work is the development of a model that allows to perform numerical simulations of atmospheric flows over a complex terrain through a CFD model considering the momentum and energy equations, through the use of the commercial software Ansys Fluent. It was concluded that the presence of the forest causes a modification in the velocity profile due to the drag produced by its presence, and the values could be used in a mathematical model to obtain the fire rate of spread and fire line intensity. Through the combustion simulations it was also possible to verify that high temperatures can result in convection currents with high speeds.

**Keywords:** Wildfires, CFD, Ansys-Fluent, ROS

### 1. Introduction

The occurrence of wildfire, when destructive, happens mostly as a result of human irresponsibility with their finite resources, resulting in intense negative repercussions.

Models to describe the wildland fire spread behavior across the landscape can be organized in three main categories [1]: theoretical, empirical and semiempirical models. From this point of view, and based on the literature review, an algorithm was built, involving both a semiempirical surface model carried by [2] and two crown models. One of the models is semiempirical developed by Van Wagner [3], and the other developed by Rothermel [4]. In either case, the aim is to estimate the fire rate of spread (ROS) and fireline intensity, according to certain parameters, correctly identified and quantified regarding the fuel type, terrain, and weather conditions.

To understand fire behavior, one of the main goals in this study is to analyze how the airflow behaves when the combustion processes are accounted for, using a computational fluid dynamics (CFD) model along with the implementation of mathematical models of fire

spread, considering the topography and the type of fuel in the forest [5][6][7].

Similar to the works performed by [8][9][10][11][12], the impacts of the forest canopy can be represented in CFD simulations by including source and sink terms in the governing equations for momentum and turbulent transport, within a sub-domain representing the vegetation. For the combustion simulations, the species transport model was integrated with the finite rate/eddy dissipation model for the turbulence/chemistry interaction.

Through this work, it will be possible to develop a model capable of studying the behavior of fire in a flat terrain with a forest, considering energy and the associated combustion processes, increasing the knowledge that so far is empirical. The main contribution is to expand the knowledge of forest fires in order to enhance the tools that can be used to minimize their effects.

## 2. Methodology

### 2.1. Flow modeling

In this paper, the flow through and around vegetation is initially modelled. The simulations performed were based on the Reynolds averaged Navier–Stokes (RANS) equations coupled with the standard  $k$ – $\varepsilon$  turbulence model, using the commercial software ANSYS Fluent® [13].

To account for the drag generated by the vegetation, additional terms are included in the conservation equations for mean momentum and in the turbulent transport equations.

The continuity equation is shown in (1), and the momentum equation for turbulent flows is shown in equation (2) [11]:

$$\frac{\partial(\rho u_i)}{\partial x_i} = 0 \quad (1)$$

$$\frac{\partial(\rho u_i u_j)}{\partial x_j} = -\frac{\partial p}{\partial x_i} + \frac{\partial}{\partial x_j} \left[ \left( \mu \left( \frac{\partial u_i}{\partial x_j} + \frac{\partial u_j}{\partial x_i} \right) - \frac{2}{3} \delta_{ij} \frac{\partial u_l}{\partial x_l} \right) \frac{\partial k}{\partial x_j} \right] + \frac{\partial}{\partial x_j} - (\rho \overline{u'_i u'_j}) + S_{u_i} \quad (2)$$

Here,  $\rho$  is the air density;  $u_i$  (or  $u_j$ ) is the ensemble-averaged velocity component of the fluid;  $p$  is the static pressure,  $\mu$  is the dynamic viscosity;  $\delta_{ij}$  is the Kronecker delta;  $(-\rho \overline{u'_i u'_j})$  the Reynolds stress modeled due to turbulence; and  $S_{u_i}$  represents the absorption of momentum due to the aerodynamic drag of vegetation elements, defined in equation (3), where  $C_2$  parameter, which represents the forest resistance, is specified in equation (4):

$$S_{u_i} = -\rho C_2 |U| u_i \quad (3)$$

$$C_2 = c_d LAD \quad (4)$$

$LAD$  is the leaf area density, generally considered constant with height and, in this case, has a value of  $0.15 \text{ m}^2/\text{m}^3$ , which is representative of a dense forest.  $c_d$  is the dimensionless drag coefficient of vegetation, set to 0.2 in CFD modeling to represent an average value instead of a specific species value [8], and  $U$  is the free stream wind velocity.

The turbulent transport can be modeled through the  $k$ – $\varepsilon$  RANS model with standard wall treatment. Reynolds averaging results in the introduction of source terms for the equations of the turbulent kinetic energy  $k$ , and turbulent dissipation rate  $\varepsilon$ , of the turbulence model, represented in equations (5) and (6) [9]:

$$\frac{\partial(\rho k u_i)}{\partial x_i} = \frac{\partial}{\partial x_j} \left[ \left( \mu + \frac{\mu_t}{\sigma_k} \right) \frac{\partial k}{\partial x_j} \right] + G_k - \rho \varepsilon + S_k \quad (5)$$

$$\frac{\partial(\rho \varepsilon u_i)}{\partial x_i} = \frac{\partial}{\partial x_j} \left[ \left( \mu + \frac{\mu_t}{\sigma_\varepsilon} \right) \frac{\partial \varepsilon}{\partial x_j} \right] + C_{\varepsilon 1} \frac{\varepsilon}{k} G_k - C_{\varepsilon 2} \rho \frac{\varepsilon^2}{k} + S_\varepsilon \quad (6)$$

$S_k$  and  $S_\varepsilon$  are, respectively, the source and sink terms for  $k$  and  $\varepsilon$ ;  $G_k$  is the production of  $k$ ;  $\mu_t$  is the turbulent viscosity;  $\sigma_k$  and  $\sigma_\varepsilon$  are the turbulent Prandtl numbers for  $k$  and  $\varepsilon$ ; and  $C_\mu$ ,  $C_{\varepsilon 1}$  and  $C_{\varepsilon 2}$  are the turbulence model constants. Assuming a neutral atmospheric condition, the ideal modified turbulence model constants for an atmospheric flow are shown in Table 1 [14]:

**Table 1.** Turbulence model constants [14].

$C_\mu$	$\sigma_k$	$\sigma_\varepsilon$	$C_{\varepsilon 1}$	$C_{\varepsilon 2}$
0.033	1	1.835	1.44	1.92

The source terms added in the  $k$ – $\varepsilon$  turbulence equations are described in equation (7) and (8):

$$S_k = \rho C_2 |U| (\beta_p |U|^2 - \beta_d k) \quad (7)$$

Where  $\beta_p = 0.99$  is the fraction of mean kinetic energy converted into  $k$  by means of drag, and  $\beta_d = 3$  is the dimensionless coefficient for the turbulence cascade short-circuiting [9][11].  $S_\varepsilon$  is modelled by equation (8):

$$S_\varepsilon = \rho C_2 |U| \varepsilon \left( \frac{C_{\varepsilon 4} \beta_p |U|^2}{k} - C_{\varepsilon 5} \beta_d \right) \quad (8)$$

$C_{\varepsilon 4} \in C_{\varepsilon 5}$  are the turbulence model constants and their values are, respectively, 1.8 and 1.5 [10].

### Combustion modeling

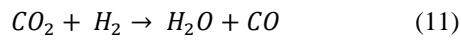
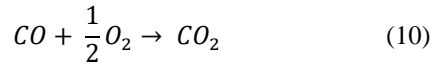
The 2D mathematical representation of the energy in steady state is presented in equation (9), solved for flows involving heat transfer or compressibility [15]:

$$\rho c \left( u_i \frac{\partial T}{\partial x_i} \right) = k \frac{\partial^2 T}{\partial x^2} + \frac{\partial u_j \tau_{ij}}{\partial x_i} + S_E \quad (9)$$

Here, the left term on the equation represents the energy transport by convection, with  $T$  corresponding to the temperature and  $c$  to the specific heat; the first term on the right side of the equation represents the transport by diffusion, with  $k$  corresponding to the thermal conductivity coefficient; the second term corresponds to the energy generated by the stress forces, with the suffix notation  $\tau_{ij}$  used to indicate the direction of the viscous stresses; and  $S_E$  represents the energy source term.

Due to combustion, there is a wide variety of pollutants released during a wildfire: greenhouse gases, such as carbon dioxide ( $\text{CO}_2$ ), methane ( $\text{CH}_4$ ), nitrous oxide ( $\text{N}_2\text{O}$ ), photochemical reactive compounds such as carbon monoxide ( $\text{CO}$ ) and nitrogen oxides ( $\text{NO}_x$ ), and, finally, particulate matter (PM) [16]. From

previous analysis of a study conducted by [16], who set out to record emission factor data by geographical zones (tropical, temperate, and boreal) and vegetation types (forest/savanna and grassland), it is possible to determine the different types of emissions from biomass burning in different regions. According to the authors, the highest emissions are recorded for  $CO_2$  and  $CO$ , followed by  $PM_{2.5}$  and  $CH_4$ . The project developed will be based on equations (10) and (11) presented, focusing essentially on the release of  $CO_2$  and  $CO$ :



To simulate the combustion, a species transport model was chosen. For the turbulence-chemistry interaction, the hybrid Finite Rate/Eddy Dissipation model (FR/EDM) was selected to analyze the volatiles released, which includes the rate reaction of both the finite rate (FR) and the eddy dissipation model (EDM).

Different factors must be initially determined, ranging from the computational domain features, boundary conditions, and solver configuration to the discretization scheme, in order to construct a CFD technique capable of modeling wind flow through and around a forest in the atmospheric boundary layer (ABL), considering the combustion reactions and ignition source.

## 2.2. Geometry and Mesh

Initially, a rectangular domain was created, represented in Figure 1, with a length of 250 m to allow the full development of the flow. To represent the forest, a rectangle was included in the domain with a length of 100 m and a height of 20 m.

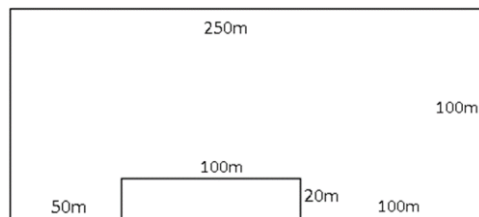


Figure 1. Domain dimensions.

The mesh was completely structured using square elements, resulting in a total domain with 156,250 elements and an element size of 0.4 m. To evaluate if a mesh is well structured, three quality parameters were studied: skewness, orthogonal quality, and aspect ratio. Through their analysis, the mesh was considered excellent.

## 2.3. Boundary Conditions

In most cases, an atmospheric boundary layer (ABL) has only one boundary, the ground. However, in fluid simulation, boundary conditions must be defined in all directions of the domain in order to solve the problem satisfactorily. Table 2 summarizes the boundary conditions used for all simulations.

Table 2. Boundary conditions.

Element	Boundary condition
Inlet	Velocity inlet
Bottom	Wall
Top	Outflow
Outlet	Outflow

Two different cases were simulated. Figure 2 represents the 2D domain used for the case without energy, case A, and Figure 3 represents the domain that accounts for the combustion reactions and includes an ignition source, case B. The combustion zone in Figure 3 is defined as the zone immediately above the species inlet, the first 25 % area of the beginning of the forest.

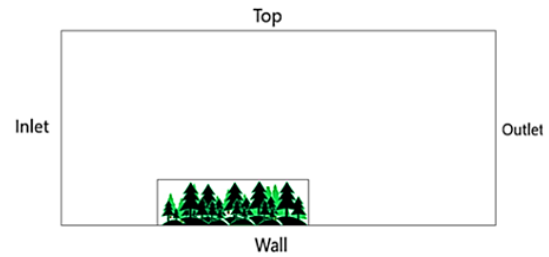


Figure 2. Case A domain scheme.

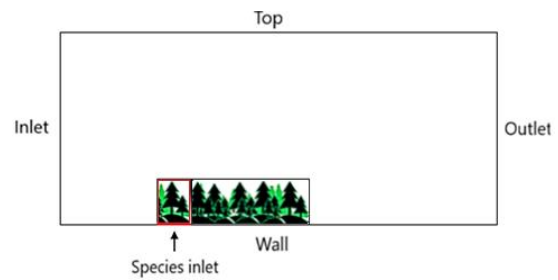


Figure 3. Case B domain scheme.

### Flow inlet

For the flow inlet, and considering the consistency between the input profiles, the wall functions, the computational grid and the turbulence model, the equations defined by [17] were used. The logarithmic velocity profile is represented by Equation (12), the turbulent kinetic energy by Equation (13), and the turbulent dissipation rate by Equation (14):

$$U = \frac{u_*}{\kappa} \ln \left( \frac{z_{ref} + z_0}{z_0} \right) \quad (12)$$

$$k = \frac{u_*^2}{\sqrt{C_\mu}} \quad (13)$$

$$\varepsilon = \frac{u_*^3}{\kappa(z + z_0)} \quad (14)$$

$\kappa$  is known as the von Karman constant with a mean value of 0.41,  $z_0$  is the roughness length with a chosen value of 0.01,  $u_*$  is the friction velocity, calculated by assuming a wind velocity of 4 m/s at the top of the ABL, resulting in a value of 0.178 m/s.

### Species inlet

The data used in this section were based on a literature review, in particular the experimental work of [18], regarding the combustion kinematics of forestry biomass, as well as the (semi or quasi) empirical models of [5,7]. Other authors [2,3], provided data for the fire rate of spread (ROS) and intensity, given a set of input values such as forest density and wind speed. To determine the species inlet velocity, one requires to estimate the amount of biomass,  $m_{biomass}$ , that will be burned in the combustion zone. This can be done by multiplying the biomass density,  $\rho_{biomass}$ , set to the medium value of 400 kg/m<sup>3</sup>, by the chosen combustion volume (where the ignition and combustion is initially set to occur),  $V_{combustion}$  equal to 400 m<sup>3</sup>, resulting in 160,000 kg of biomass. With the use of equation (15), the biomass flow rate,  $\dot{m}_{biomass}$ , is obtained.

$$\dot{m}_{biomass} = \frac{m_{biomassa}}{\Delta t} \quad (15)$$

Where  $\Delta t$  corresponds to the amount of time that the biomass takes to burn in the combustion zone, and it is equal to 694.4 s. This value was obtained through the use of the empirical model as described in [5][7], using the data provided for density and velocity values of case A simulations. From the mathematical model, the fire ROS is extracted at  $x=75$  m. Dividing the resulting fire ROS by the distance, the result will be the amount of time that biomass takes to burn.

The last formula needed to calculate the species velocity is represented in equation (16):

$$U_{biomass} = \frac{\dot{m}_{biomass}}{\rho_{gases} V_{combustion}} \quad (16)$$

Where  $\rho_{gases}$  represents the density of the gases released from the combustion reactions, and it is equal to 0.33 kg/m<sup>3</sup> [18]. Substituting all the parameters results in a species velocity of 1.33 m/s.

The input mass fractions of all species are represented in Table 3, based on the combustion experiments performed by [18].

**Table 3:** Species input mass fractions.

Species	Mass fraction
Carbon monoxide (CO)	0.28
Carbon dioxide (CO <sub>2</sub> )	0.36
Water (H <sub>2</sub> O)	0.3
Hydrogen (H <sub>2</sub> )	0.006
Oxygen (O <sub>2</sub> )	0.04

Since the FR/EDM is being used for the turbulent-chemistry interaction, the use of the functionality of the patch is suggested to simulate the ignition source, because this ignition is the equivalent of a spark. In this case, a patch can connect a hot temperature, set to 1,300 K (1,027 °C), into a specific region of the ANSYS Fluent® domain that contains sufficient fuel/air mixture for ignition to occur, which in this case was the combustion zone [13].

### 2.4. Solver configurations

The method used by ANSYS Fluent® as the discretization method to solve equations is the finite volume method (FVM).

The solver chosen was the coupled algorithm pressure-based solver, considering the model availability, solver performance for the flow conditions, the size of the mesh, and the available memory on the computer [13]. For case A, solved in steady mode, the method selected was the SIMPLE algorithm. For case B, solved in transient state, the PISO option is recommended by other authors. For both cases, the selected settings are presented in Table 4.

**Table 4.** Spatial discretization scheme.

Parameter	Option chosen
Gradients	Least Squares Cell Based
Pressure	PRESTO!
Momentum	Second Order Upwind
Turbulent kinetic energy	
Turbulent dissipation rate	
H <sub>2</sub> O*	
O <sub>2</sub> *	
CO <sub>2</sub> *	
CO*	
H <sub>2</sub> *	Second Order Upwind
Energy*	

\*combustion cases

### 3. Results and Discussion

#### 3.1. Flow field results

To assess the influence of the energy, the model was firstly simulated without accounting for the energy, referred to as case A. The results of the velocity vectors are presented in Figure 4.

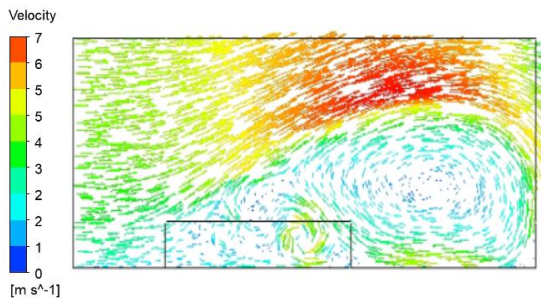


Figure 4. Case A: velocity vectors results.

From these results, it can be concluded that the presence of forestry is a strong component that affects the airflow and that it should be considered as a crucial factor when modeling fire propagation.

Regarding the recirculation of the wind presented inside and outside the canopy (commonly called vortices), this phenomenon was also verified by [19], who stated that recirculation zones along the forest-to-clearing canopy edge are time-intermittent, consistent with earlier studies. At the forest-to-clearing canopy edge, the recirculation and exit flow alternate in the spanwise direction, and one of the hypotheses formulated is that the volume fraction occupied by these two different flow structures must vary with the forest *LAD* (which is the parameter where the forest type is differentiated, if sparser or denser types of forests).

To analyze the inlet profiles of the velocity in the *x*-direction, four different horizontal distances downstream of the inlet were selected in the results, and Figure 5 was created with the velocity profile.

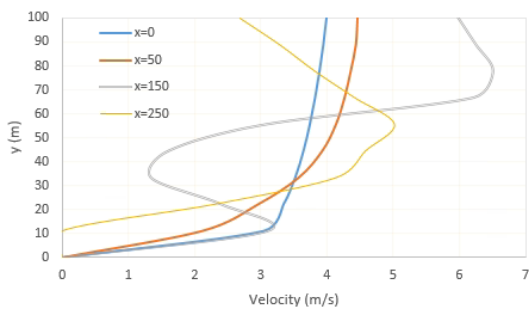


Figure 5. Case A: vertical velocity profile, at  $x=0, 50, 150, 250$  m.

It is verified that nearly after the top of the forest, there is an overall higher wind speed, which can be explained by more momentum being transported above the canopy, with the exception of the values registered at  $x=150$  m (end of forest), since they capture the vortex created.

Figure 6 depicts the streamwise velocity at the top edge of the vegetation, presenting the different profiles and the influence of the presence of the rectangular homogeneous vegetation.

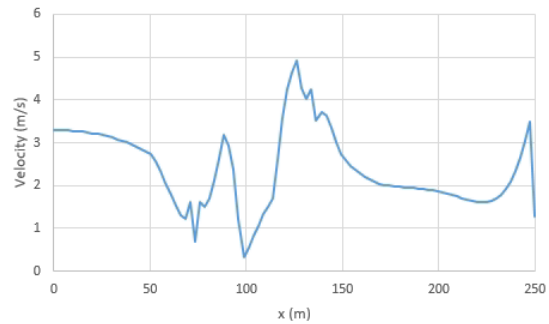


Figure 6: Case A: streamwise velocity, at the top edge of the vegetation ( $y=20$  m).

The forest clearly represents an interference on the airflow, which can traduce itself in an increase of turbulence and the creation of recirculating zones of air, leading to variation of the velocity values presented.

The greater variation of the velocity values can also be due to the fact that it is being simulated as a dense forest, which leads to a higher blockage of airflow.

#### 3.2. Combustion results

For the combustion analysis, results of velocity, temperature, and species contours were extracted.

In Figure 7 the velocity contours of case B are presented, followed Table 5, which presents the maximum velocity values registered at the different times of simulation.

It can be observed from the first analysis that the velocity values are significantly higher than those obtained from the simulation without combustion. This could be due to the high combustion temperature since the software calculates the velocity values according to the ideal gases' equation, which implies that when the temperature rises, it causes a density drop, which will increase the velocity values. Also, the velocities presented are punctual values in a single cell, and high temperatures lead to the creation of convection currents, which in turn lead to higher velocity.

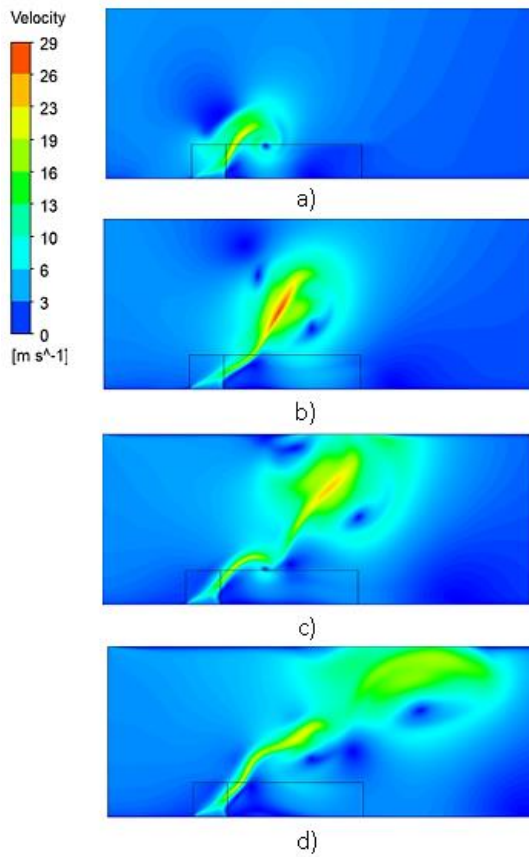


**Figure 7.** Case B: velocity contours: a)  $t=5s$ , b)  $t=10s$ , c)  $t=15s$ , and d)  $t=20s$ .

**Table 5.** Maximum velocity values for case B.

Time (s)	$V_{max\ dense}$ (m/s)
5	24.016
10	27.621
15	24.020
20	21.520

In Figure 8, the temperature contours of case B are presented, followed by Table 6, which presents the maximum temperature values registered at the different times of simulation. To corroborate the findings referred above, it is expected that, in general, the zones of higher velocities correspond to the zones of higher temperatures.

By comparing Figure 7 and Figure 8, and to support the previous conclusion, it is clear how velocity and temperature behave in a complementary manner since they present similar behavior.

The ascending convection current caused by the high temperature could be the main reason for the higher velocity values registered.

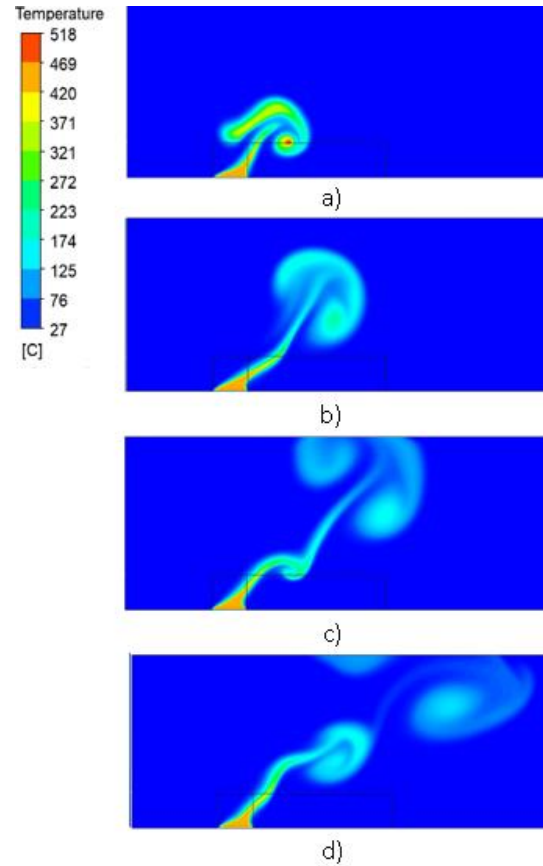


**Figure 8.** Case B: temperature contours: a)  $t=5s$ , b)  $t=10s$ , c)  $t=15s$ , and d)  $t=20s$ .

**Table 6.** Maximum temperature values for case B.

Time (s)	$T_{max}$ (°C)
5	523.26
10	465.547
15	466.174
20	466.285

To evaluate the species release, Figure 9 was created, displaying the species contours for the two main components released in a wildfire event: carbon dioxide,  $CO_2$ , and carbon monoxide,  $CO$ .

The values for the different species obtained were  $CO_2 = 0.404$  and  $CO = 0.304$ . Through the analysis of Figure 9, it can be concluded that the  $CO$  was successfully converted into  $CO_2$ , and that both reactions are being well simulated since not all  $CO$  is converted due to the second reaction presented in equation (11).

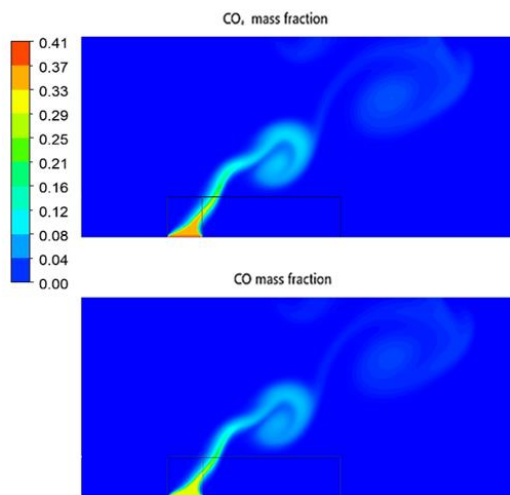


Figure 9. Case B: CO<sub>2</sub> and CO species contours,  $t=20$

#### 4. Conclusions

The overall objective of this work was accomplished, which was to develop a modeling approach that was able to reproduce to some extent the thermochemical fire behavior characteristics with canopy involvement. From the flow modeling simulation, case A, despite the absence of validation, by the analysis of the different results presented, it is feasible to affirm that the model is capable of simulating airflow within and around forests, demonstrating the creation of vortices which in a wildfire could lead to hot spots.

From the combustion simulations, case B, it can be concluded that when heat is applied to a fluid and its density varies with temperature, it is possible that a flow is induced due to the resultant force of gravity acting on density variations, leading to ascendent convection currents and high simulation values of velocity.

This work aims to present the overall behavior and study key elements that drive wildfires rather than provide a thorough assessment of the whole area of wildfire research.

#### 5. Acknowledgements

This work has been supported by FCT, the Portuguese Foundation for Science and Technology, within the Project Scope: PCIF/GRF/0141/2019 "O3F – An Optimization Framework to reduce Forest Fire", and within the R&D Units Project Scope UIDB/00319/2020 (ALGORITMI) and UIDP/04077/2020 (MEtRICs). Furthermore, João Silva would like to also express his acknowledgment for the support given by the FCT through the PhD grant SFRH/BD/130588/2017.

#### 6. References

- [1] Pastor, E., Zárate, L., Planas, E., and Arnaldos, J., 2003, "Mathematical Models and Calculation Systems for the Study of Wildland Fire Behaviour," *Prog. Energy Combust. Sci.*, **29**(2), pp. 139–153.
- [2] Rothermel, R., 1972, "A Mathematical Model for Predicting Fire Spread," *USDA For. Serv. Res. Pap.*, p. 46.
- [3] Wagner, C. E. Van, 1977, "Conditions for the Start and Spread of Crown Fire," *Can. J. For. Res.*, **7**(1), pp. 23–24.
- [4] Rothermel, R. C., 1991, "Predicting Behavior and Size of Crown Fires in the Northern Rocky Mountains," *USDA For. Serv. Intermt. Res. Stn.*, **438**(January), p. 46.
- [5] Marques, J., Silva, J., Oliveira, G., Teixeira, S., and Teixeira, J., 2021, "Implementation of a Forest Fire Propagation Model," *8th International Conference on Energy, Sustainability and Climate Crisis*.
- [6] Gonçalves, I., Pinto, F., Silva, J. P., Alvelos, F., Teixeira, J. C., Tavares, T., and Teixeira, S., 2022, "Modelling the Effect of Forestry Using a Simplified CFD Model," *French German Portuguese Conference on Optimization (2022)*.
- [7] Gonçalves, I., Marques, J., Silva, J. P., Alvelos, F., Teixeira, J. C., Tavares, T., and Teixeira, S., "Development of CFD Model to Study the Spread of Wildfires," *ASME 2022 International Mechanical Engineering Congress and Exposition*, accepted.
- [8] Buccolieri, R., Santiago, J. L., Rivas, E., and Sanchez, B., 2018, "Review on Urban Tree Modelling in CFD Simulations: Aerodynamic, Deposition and Thermal Effects," *Urban For. Urban Green.*, **31**(July 2017), pp. 212–220.
- [9] Zeng, F., Lei, C., Liu, J., Niu, J., and Gao, N., 2020, "CFD Simulation of the Drag Effect of Urban Trees: Source Term Modification Method Revisited at the Tree Scale," *Sustain. Cities Soc.*, **56**(January).
- [10] Desmond, C. J., Watson, S. J., Aubrun, S., Ávila, S., Hancock, P., and Sayer, A., 2014, "A Study on the Inclusion of Forest Canopy Morphology Data in Numerical Simulations for the Purpose of Wind Resource Assessment," *J. Wind Eng. Ind. Aerodyn.*, **126**, pp. 24–37.
- [11] Santiago, J. L., Martín, F., and Martilli, A., 2013, "A Computational Fluid Dynamic Modelling Approach to Assess the Representativeness of Urban Monitoring Stations," *Sci. Total Environ.*, **454–455**, pp. 61–72.
- [12] Santiago, J. L., Buccolieri, R., Rivas, E., Calvete-Sogo, H., Sanchez, B., Martilli, A.,

- Alonso, R., Elustondo, D., Santamaría, J. M., and Martin, F., 2019, “CFD Modelling of Vegetation Barrier Effects on the Reduction of Traffic-Related Pollutant Concentration in an Avenue of Pamplona, Spain,” *Sustain. Cities Soc.*, **48**(April), p. 101559.
- [13] ANSYS Inc., 2013, *ANSYS Fluent Theory Guide*.
- [14] Costa Silva, D. M., 2021, “CFD Analysis of the Air Flow Through Horizontal Axis Wind Turbines,” University of Minho.
- [15] Versteeg, H. K., and Malalasekera, W., 1995, *An Introduction to Computational Fluid Dynamics- the Finite Volume Method*, Longman Malaysia.
- [16] Urbanski, S. P., Hao, W. M., and Baker, S., 2008, “Chemical Composition of Wildland Fire Emissions,” *Developments in Environmental Science*, pp. 79–107.
- [17] Richards, P. J., and Norris, S. E., 2012, “Appropriate Boundary Conditions for a Pressure Driven Boundary Layer,” *Proceedings of the 18th Australasian Fluid Mechanics Conference, AFMC 2012*, pp. 1–4.
- [18] Silva, J., Teixeira, S., and Teixeira, J. C., 2022, “An Experimental Setup to Study the Fundamental Phenomena Associated With Biomass Combustion,” *ASME 2022 International Mechanical Engineering Congress and Exposition*.
- [19] Cassiani, M., Katul, G. G., and Albertson, J. D., 2008, “The Effects of Canopy Leaf Area Index on Airflow across Forest Edges: Large-Eddy Simulation and Analytical Results,” *Boundary-Layer Meteorol.*, **126**(3), pp. 433–460.